Nuclear Instruments and Methods in Physics Research B23 (1987) 116–119
North-Holland, Amsterdam

DOUBLE ELECTRON CAPTURE BY He-LIKE IONS: COLLISION ENERGY DEPENDENCE OF THE REACTION WINDOW

M. MACK and A. NIEHAUS

Fysisch Laboratorium, Rijksuniversiteit Utrecht, Princetonplein 5, 3584 CC Utrecht, The Netherlands

Double electron capture by the He-like ions C^{4+}, N^{5+}, O^{6+}, Ne^{8+} from the two electron targets H_2 and He is studied by spectroscopy of the autoionization electrons emitted after capture into excited states. Electron spectra are measured in a collision velocity range from 0.18 to 0.55 atomic units. The spectra are found to be due to decay of states of the type $(1s^2 3ln'l')$ and $(1s^2 4ln'l')$ into the continua $(1s^2 2l) + e^-$ and $(1s^2 3l) + e^-$, respectively. It is found that only states lying within a certain reaction window are populated. Energy position and dependence of the width of this window on the collision velocity are discussed and compared with predictions of the classical model for multiple electron capture.

1. Introduction

In this paper we report on autoionization electron spectra arising from the two electron capture process

$$\begin{aligned} A^{q+}(1s^2) + B &\rightarrow A^{(q-2)+}(1s^2 nln'l') + B^{2+} \\ &\rightarrow A^{(q-1)+}(1s^2 n''l'') + e^-(\epsilon). \end{aligned} \tag{1}$$

Spectra are reported for collisions of the He-like ions $A^{q+} \equiv C^{4+}$, N^{5+}, O^{6+}, Ne^{8+} with the two-electron targets H_2 and He, in a collision velocity range from 0.18 to 0.55 atomic units. Only on spectra for the systems N^{5+}/H_2 [1] and O^{6+}/He [2] previous information is available. However, also in these cases our data yield additional information. In our discussion of the spectra we will focus our attention on aspects which relate to the capture mechanism rather than to spectroscopic details. Especially, we will discuss the observed population distribution of the doubly excited states in terms of the predictions of a newly developed classical model for multiple electron capture [3].

Details of the experimental setup used will be published elsewhere [4]. Briefly, a well collimated beam of ions A^{q+} intersects a thermal target beam. Electrons formed in process (1) under single collision conditions are analyzed by a cylindrical mirror analyzer (CMA) whose axis is aligned with the beam. The (CMA) accepts electrons ejected into polar angles $50° \pm 2°$ for essentially all azimuthal angles, and has a resolution corresponding to $\Delta E/E = 5 \times 10^{-3}$. Due to the finite range of accepted polar angles electrons which are emitted at a well defined energy are detected as a broadened line. The width of the Doppler-broadened lines (ΔE_D) is, in our spectrometer, approximately

$$\Delta E_D \approx 0.25\sqrt{\epsilon\,[\mathrm{eV}]}\; V, \tag{2}$$

with ϵ the electron energy, and V the emitter velocity in atomic units. For the present study we always have $\Delta E_D > \Delta E$, whereby the Doppler-broadened line has a double peak structure. The measured spectra are intensity-corrected for ϵ-dependent transmission of the spectrometer. The correction takes into account the mode of operation of the CMA, and the transformation from the moving emitter frame to the laboratory frame. The energy scale used for the spectra is the emitter frame energy scale. This scale has not been calibrated absolutely for each spectrum, however, it was found that the absolute energies varied from spectrum to spectrum by less than ca. 100 meV, which is also the approximate accuracy of the absolute calibration obtained by measuring known autoionization lines.

2. Results

A selection of spectra is shown in fig. 1–4. The intensity scales are in arbitrary units. However, by normalizing the count rates to equal primary beam intensity and equal target gas density, approximately the same scale is obtained for all spectra.

As indicated in the spectra, we ascribe the main contributions to the population of states $(1s^2 3ln'l')$, followed by autoionization into the $(1s^2 2l\epsilon)$ continua. For the assignment of groups of peaks to states $(1s^2 nln'l')$ we used estimated binding energies of the two excited electrons. The binding energy E_1 of one electron, the one in state nl, say, is taken to be the accurate, known binding energy of one electron bound to the core $(1s^2)$ of extra charge q. The binding energy of the other electron is calculated from the Rydberg formula

$$E_2^{n'l'} \approx \frac{(q-s)^2}{2n'^2}, \tag{3}$$

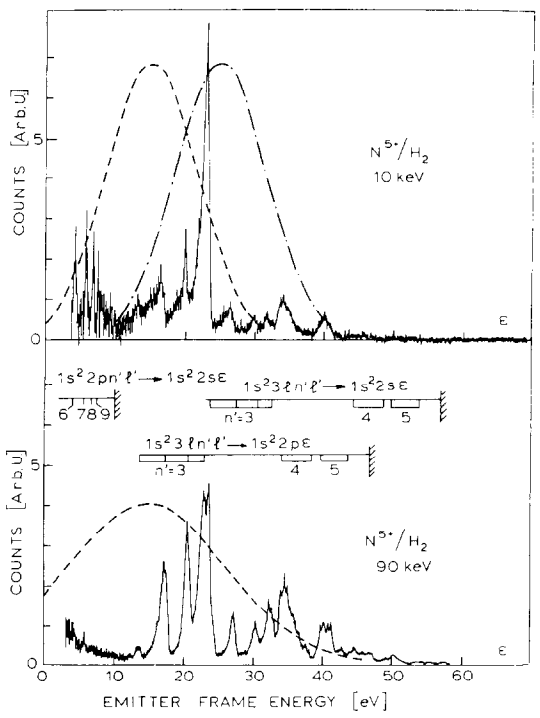

Fig. 1. N^{5+}/H_2 electron spectra at two different collision energies. Dashed lines indicate the "population window" predicted by the extended classical model. For the 90 keV spectrum the window is indicated for the case of $(1s^2 2p\epsilon l)$ final states, and for the 10 keV spectrum for the case of both $(1s^2 2p\epsilon l)$ and $(1s^2 2s\epsilon l)$ states. The intensity scale is in arbitrary units, but in the same units for all spectra shown. Our identification of peaks to autoionization transitions of the doubly excited projectile is indicated.

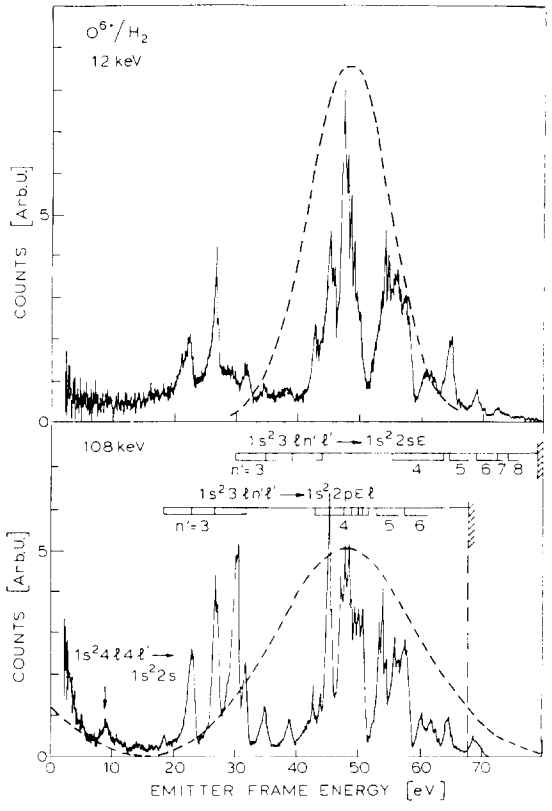

Fig. 2. O^{6+}/H_2 electron spectra at two different collision energies. Otherwise see caption of fig. 1, except that the population window is only shown for the case of $(1s^2 2p\epsilon l)$ final states.

with s the effective screening by the electron in state nl. For $n'-n \geq 1$ a good estimate is already obtained for $s \approx 1$. For $n' = n$ we used s-values suggested by Slater [5]. For example, we obtain for N^{5+} $(1s^2 3s^2)$ the following binding energies: $E_1^{3s} = 41.3$ eV, $E_2^{3s} = (5 - 0.35)^2/18$ (a.u.) $= 32.7$ eV. In terms of these binding energies the electron energy corresponding to the autoionization process $(1s^2 3s^2) \rightarrow (1s^2 2p)$ is $IP(q) - E_1^{3s} - E_2^{3s} - E(1s^2 2s \rightarrow 1s^2 wp) = 97.9 - 41.3 - 32.7 - 10)$ eV $= 13.9$ eV. As seen in fig. 1, this energy coincides with the position of the lowest peak of the $(3l3l')$-group of peaks. Using $s = 1$ for the calculation of E_2^{4s} by relation (3), we obtain for electrons corresponding to the autoionization $(1s^2 3s4s)$–$(1s^2 2p)$ the energy 33 eV, where, according to our assignment, the lowest peak of the $(1s^2 3l4l')$-group of peaks is positioned. In the N^{5+}/H_2 spectrum at low collision energy (fig. 1) also a series of Rydberg states of the configuration $(1s^2 2pn'l')$, which decay to $(1s^2 2s\epsilon)$, is observed. Such Rydberg states are also observed for C^{4+}/H_2. In cases where states close to the series limit $(1s^2 3l\infty l')$ are populated with significant probability – such as for the system Ne^{8+}/H_2 and for O^{6+}/H_2 at high collision velocity – also autoionization of states $(1s^2 4ln'l')$ into the continua $(1s^2 3l\epsilon)$ are observed. The variation of the spectra with collision energy may be characterized as a broadening of a "population window" whose energy position does not change. This is clearly seen in figs. 1 and 2 for the systems N^{5+}/H_2 and O^{6+}/H_2. The main effect of the change of the target is that the population window moves to higher excitation energies of the doubly excited states when going from He to H_2. This is demonstrated in fig. 3 for the Ne^{8+} spectra. The spectra further show that the cross section for population of autoionizing states – represented by the area under the observed peaks in the spectra – varies considerably from system to system. Finally, we point out that the widths of some of the single autoionization lines of the $(1s^2 3l3l')$-group of all spectra are considerably broader than the lines of the $(1s^2 3ln'l')$-groups for $n' > 3$.

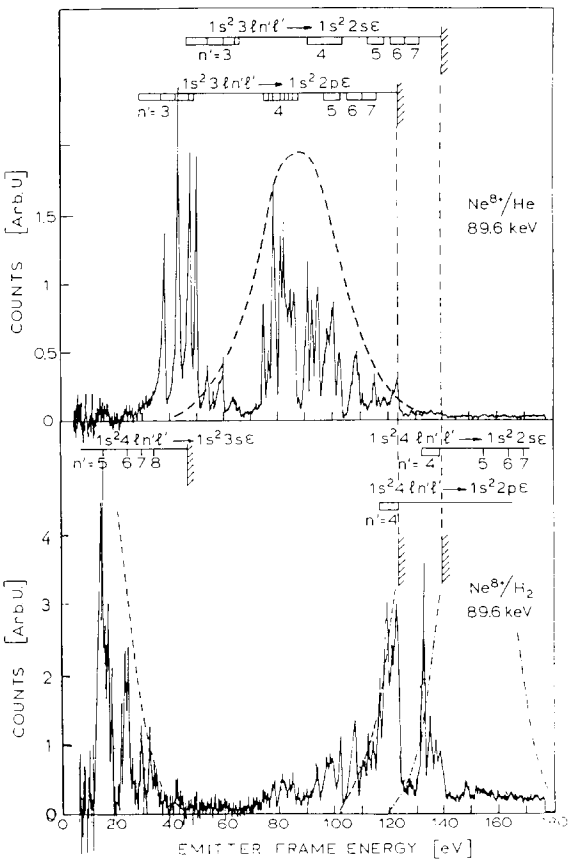

Fig. 3. Ne^{8+}/H_2 and Ne^{8+}/He electron spectra at the same collision energy. For the Ne^{8+}/H_2 spectrum the low energy population window is shown for both ($1s^2 2p\epsilon l$) final states (- - -) and ($1s^2 2s\epsilon l$) final states (– · –). States lying within the high energy wing of the population window decay to ($1s^2 3s\epsilon$) final states and yield low energy electrons (- - -). Otherwise see caption of fig. 1.

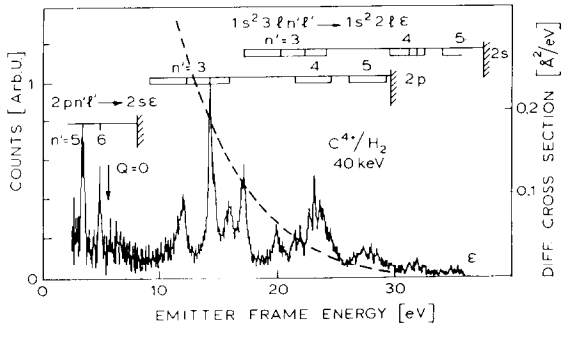

Fig. 4. C^{4+}/H_2 spectrum at 40 keV collision energy. Note that the autoionizing lines lie in the wing of the predicted population window, and that the measured cross sections corresponding to these lines are considerably lower than for systems where the lines lie in the center of the population window.

3. Discussion

It would be beyond the scope of this paper to discuss in detail all the features pointed out. We will concentrate on a few aspects. One of us [3] has formulated an extended classical model for multiple electron capture, which is based on the "overbarrier criterion" used previously in a model for single capture [6]. The extended model – which does not contain free parameters – predicts in its classical form the binding energy of each of the captured electrons. In the case of double capture, from these binding energies (E_1, E_2) the most probable energy position ϵ_0 of autoionization lines can be calculated as

$$\epsilon_0 = \mathrm{IP}(q) - E_1 - E_2 - E_*, \tag{4}$$

where IP(q) is the energy needed for the ionization $A^{(q-1)+} \rightarrow A^{q+}$, and E_* the excitation energy above the ground state of the ion $A^{(q-1)+}$ after the autoionization $A^{(q-2)+} \rightarrow A^{(q-1)+} + e^-$. Taking into account that the overbarrier criterion is "uncertain" because of the time–energy uncertainty relation, the classical prediction of a fixed value of each binding energy is replaced by the prediction of a distribution (Gaussian) of values. In this way also ϵ_0 is replaced by a Gaussian centered at ϵ_0. The width of the Gaussian is proportional to the square root of the collision velocity, and depends on the collision system. In each of the spectra shown, the predicted Gaussian is indicated for the case of autoionization into ($1s^2 2p\epsilon$), which contributes predominantly in most cases, as can be seen from the identification of peaks. In case of N^{5+}/H_2 (fig. 1) and of Ne^{8+}/H_2 (fig. 3), where also autoionization into ($1s^2 2s\epsilon$) is significant, the corresponding Gaussian – shifted by the transition energy $1s^2 2p \rightarrow 1s^2 2s$ – is also shown.

Comparison of the predicted "population window" – the Gaussian – with the observed one shows good qualitative agreement regarding position, width, and energy dependence. Also the variation from system to system of the observed cross sections seems to be explained by the availability of states within the predicted window. The very low cross sections for C^{4+}/H_2 and Ne^{8+}/H_2 appear to be caused by the fact that states are only available in the wings of the Gaussian. In the case of Ne^{8+}/H_2 we have an interesting example of the condition that the Gaussian for the ($1s^2 2s$) final state extends far into the continuum ($1s^2 3l\epsilon$), where states of the configuration ($1s^2 4l n'l'$) lie. It is seen that these states are actually populated in the predicted region, leading to the low energy peaks of the spectrum by transitions to ($1s^2 3l\epsilon$). The O^{6+}/H_2 and N^{5+}/H_2 spectra show that, if by diabatic broadening the population window extends beyond the ($1s^2 3l\infty l'$) limit, at high collision energies, a low energy continuous spectral component arises which resembles that part of the

Gaussian which extends beyond the $(1s^2 3l \infty l')$ limit, and therefore probably has to be attributed to the process of capture plus ionization.

The broad asymmetric shape of peaks present in all $(1s^2 3l 3l')$-groups we ascribe to the PCI effect [7]. A crude evaluation yields lifetimes of the order of a few fs (1 fs = 10^{-15} s). Due to overlap of the broadened and shifted peaks at low collision velocities, interference effects arise, which lead to a distortion of the individual lines and to additional oscillatory structure. Indications thereof are visible in the low energy spectra of N^{5+}/H_2 and O^{6+}/H_2. More detailed measurements, not shown here, show the PCI effects more clearly. The lifetimes of the $(1s^2 3ln'l')$ states are at least of the order of 10 fs.

Finally we shortly comment on the population of Rydberg states of the type $(1s^2 2pnl)$ which decay to $(1s^2 2s\epsilon)$ and give rise to the series of peaks below 10 eV (see figs. 1 and 4). The population of these states deserves special mention because the large difference in binding energies of the two electrons is in apparent contradiction to the independent electron model of double capture. In fact, also the extended classical model [3] predicts similar principal quantum numbers for the two captured electrons. The authors of ref. [2] therefore conclude that a "correlated capture" is responsible for the population of these states. Although one can, at the moment, not exclude that such "correlated capture" processes occur, we believe that the available evidence is not conclusive. Other reasons may be responsible. For instance, after an uncorrelated capture there may arise strong configuration interaction during the collision, when the two electrons are in similar molecular orbitals, leading to an admixture of orbitals which upon separation give rise to the population of the $2pnl$ Rydberg states. In fact, the way in which we observe in our spectra the predicted population window "to be filled" by states $(3ln'l')$, with (n') extending to large numbers, seems best interpreted if one assumes that the sum of the binding energies of the captured electrons may to a certain extent be redistributed within the limits given by the uncertainty relation.

References

[1] A. Gleizes, P. Benoit-Cattin, A. Bordenave-Montesquieu, S. Dousson and D. Hitz, 14th ICPEAC abstracts, Palo Alto (1985) p. 464.
[2] N. Stolterfoht, C.C. Havener, R.A. Phaneuf, J.K. Swenson, S.M. Shafroth and F.W. Meyer, Phys. Rev. Lett. 57 (1986) 74.
[3] A. Niehaus, J. Phys. B19 (1986) 2925.
[4] M. Mack and A. Niehaus, to be published.
[5] J.C. Slater, Phys. Rev. 36 (1930) 57.
[6] H. Ryufuku, K. Sasaki and T. Watanabe, Phys. Rev. A21 (1980) 745.
[7] R. Morgenstern, A. Niehaus and U. Thielmann, J. Phys. B10 (1977) 1039.